Article

Cell

A Biogenesis Step Upstream of Microprocessor Controls miR-17∼92 Expression

Graphical Abstract

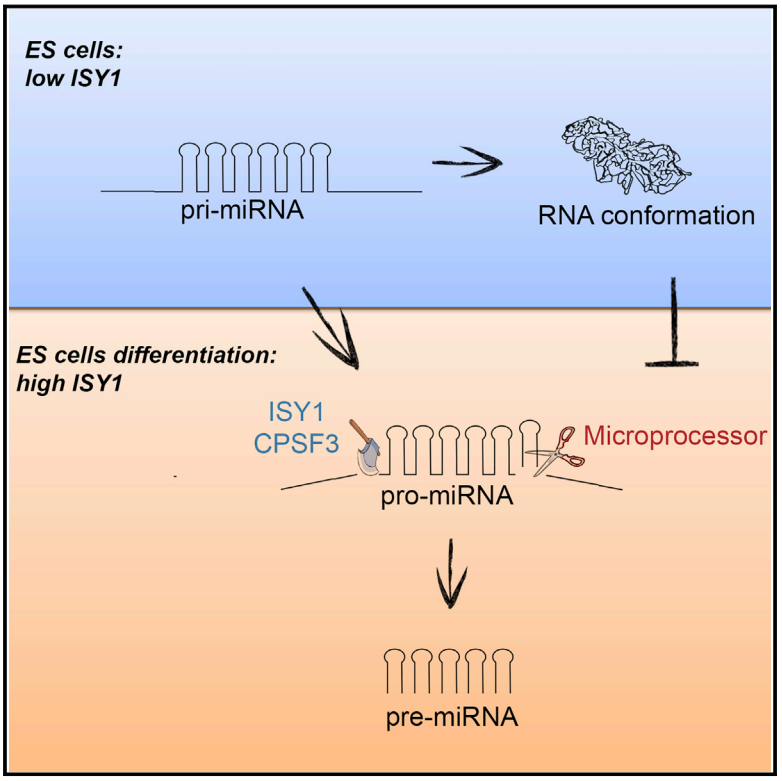

Authors

Peng Du, Longfei Wang, Piotr Sliz, Richard I. Gregory

Correspondence

rgregory@enders.tch.harvard.edu

In Brief

cis-acting sequences within a cluster-derived pri-miRNA can dynamically regulate expression of the constituent miRNAs and allow the uncoupled production of individual miRNAs from within the cluster during development.

Highlights

- Pri-miR-17∼92 adopts an RNA conformation that selectively blocks Microprocessor
- Pri-miR-17∼92 is processed to a progenitor-miRNA (pro-miRNA) intermediate
- The endonuclease CPSF3 and ISY1 are responsible for pro-miRNA biogenesis
- Pro-miRNA biogenesis controls miR-17∼92 expression during ESC differentiation

Accession Numbers

GSE68699

Du et al., 2015, Cell *162*, 885–899
August 13, 2015
http://dx.doi.org/10.1016/j.cell.2015.07.008

CellPress

Article

Cell

A Biogenesis Step Upstream of Microprocessor Controls miR-17∼92 Expression

Peng Du,[1,2] Longfei Wang,[2] Piotr Sliz,[2,3] and Richard I. Gregory[1,2,3,4,*]
[1]Stem Cell Program, Boston Children's Hospital, Boston, MA 02115, USA
[2]Department of Biological Chemistry and Molecular Pharmacology, Harvard Medical School, Boston, MA 02115, USA
[3]Department of Pediatrics, Harvard Medical School, Boston, MA 02115, USA
[4]Harvard Stem Cell Institute, Boston, MA 02115, USA
*Correspondence: rgregory@enders.tch.harvard.edu
http://dx.doi.org/10.1016/j.cell.2015.07.008

SUMMARY

The precise control of miR-17∼92 microRNA (miRNA) is essential for normal development, and overexpression of certain miRNAs from this cluster is oncogenic. Here, we find that the relative expression of the six miRNAs processed from the primary (pri-miR-17∼92) transcript is dynamically regulated during embryonic stem cell (ESC) differentiation. Pri-miR-17∼92 is processed to a biogenesis intermediate, termed "progenitor-miRNA" (pro-miRNA). Pro-miRNA is an efficient substrate for Microprocessor and is required to selectively license production of pre-miR-17, pre-miR-18a, pre-miR-19a, pre-miR-20a, and pre-miR-19b from this cluster. Two complementary *cis*-regulatory repression domains within pri-miR-17∼92 are required for the blockade of miRNA processing through the formation of an autoinhibitory RNA conformation. The endonuclease CPSF3 (CPSF73) and the spliceosome-associated ISY1 are responsible for pro-miRNA biogenesis and expression of all miRNAs within the cluster except miR-92. Thus, developmentally regulated pro-miRNA processing is a key step controlling miRNA expression and explains the posttranscriptional control of miR-17∼92 expression in development.

INTRODUCTION

MicroRNAs (miRNAs) are a large family of regulatory RNAs that inhibit target expression by base pairing with complementary sites in the 3′ untranslated region (3′ UTR) to promote mRNA decay and translational repression (Bartel, 2009). Canonical miRNA biogenesis involves the two-step processing of long primary miRNA transcripts (pri-miRNAs) by the Microprocessor, comprising the ribonuclease DROSHA and its essential co-factor DGCR8, to generate 50–70 nucleotide (nt) precursor miRNA (pre-miRNA) intermediates that are processed by DICER to mature ∼22 nucleotide miRNAs (Ha and Kim, 2014). Individual pri-miRNA can be expressed from distinct miRNA loci, or from introns or exons of protein coding genes. Furthermore some pri-miRNAs contain a single miRNA whereas others contain clusters of several miRNAs. Regardless, Microprocessor recognizes the hairpin structures in the pri-miRNA through the stem-loop and the stem-loop-single-stranded RNA (ssRNA) junction and specifically cleaves the double stranded RNA stem to release the 5′ and 3′ flanking segments and generate pre-miRNAs that are substrates for DICER processing (Ha and Kim, 2014).

miRNAs play critical roles in development and their dysregulation causes disease (Di Leva and Croce, 2010; Lin and Gregory, 2015; Mendell and Olson, 2012). It is increasingly well appreciated that posttranscriptional mechanisms play an important role controlling miRNA expression (Siomi and Siomi, 2010). Several Microprocessor or Dicer accessory factors and inhibitory proteins have been identified that either facilitate or inhibit distinct subsets of miRNAs. The activity of some of these factors is linked with cell-signaling pathways to afford dynamic control of the miRNA biogenesis machinery (Mori et al., 2014; Siomi and Siomi, 2010). Perturbation of these pathways can be oncogenic. One example is the posttranscriptional control of let-7 miRNA expression by the RNA-binding protein LIN28 (Thornton and Gregory, 2012).

To investigate how expression of other miRNAs might be regulated, we focused on the polycistronic miR-17∼92. Pri-miR-17∼92 encodes six (miR-17, miR-18a, miR-19a, miR-20a, miR-19b-1, and miR-92a) mature miRNAs. Haploinsufficiency of this locus causes the Feingold syndrome of microcephaly, short stature, and digital abnormalities in human patients and mouse models, whereas ablation of this locus in mouse causes perinatal lethality with heart, lung, and B cell defects (Concepcion et al., 2012; de Pontual et al., 2011; Mendell, 2008; Ventura et al., 2008). Conditional mouse knockouts highlight the importance of these miRNAs for kidney development and function and neural stem cell biology (Bian et al., 2013; Marrone et al., 2014; Patel et al., 2013). Gene amplification and increased expression of miRNAs from this cluster is observed in numerous types of cancer compared to normal tissues, and transgenic overexpression of this "OncomiR-1" promotes B cell lymphoma, T cell acute lymphoblastic leukemia (T-ALL), and retinoblastoma in mice (Conkrite et al., 2011; He et al., 2005; Mavrakis et al., 2010; Nittner et al., 2012; Sandhu et al., 2013). Individual miRNAs within this cluster promote cell proliferation, inhibit apoptosis, inhibit differentiation, and promote angiogenesis, to drive tumorigenesis (Mendell, 2008; Mu et al., 2009; Olive et al., 2009).

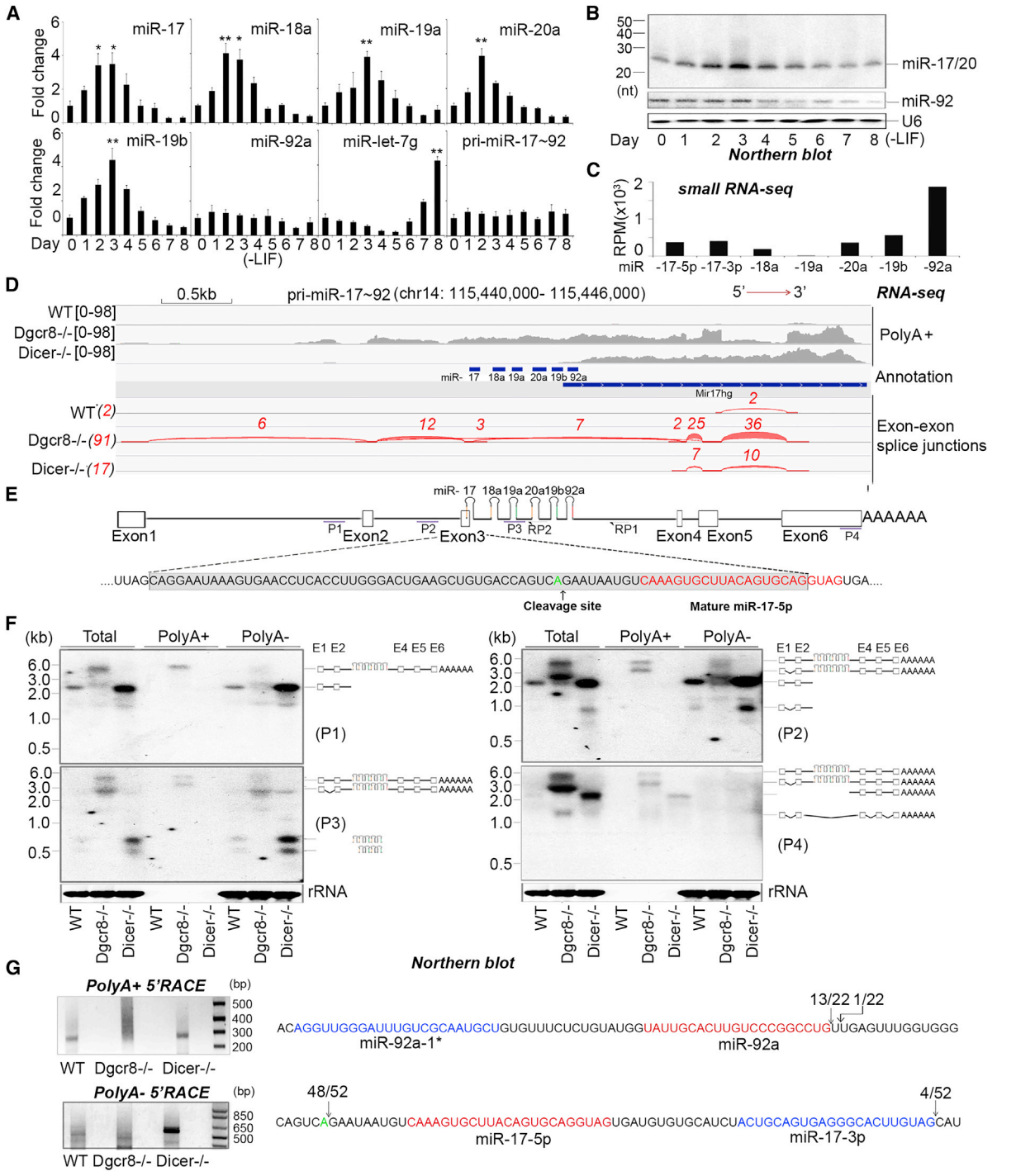

Figure 1. Posttranscriptional Regulation of miR-17∼92

(A) qRT-PCR analysis of miRNA and pri-miRNA expression in mouse ESCs over a differentiation time course. Data normalized to snoR142 (for miRNAs) and ACTIN (for pri-miRNA) and represented as mean ± SEM. *$p < 0.05$, **$p < 0.01$, Student's t test.

(B) Northern blot analysis of the RNAs from (A) using probes to detect the indicated miRNAs. U6 was used as control.

(C) Relative read number of small RNA sequences mapping to the indicated miRNAs in ESCs. RPM, reads per million.

(D) Mapping of RNA-seq cDNA sequence to the mouse miR-17∼92 locus. cDNAs were prepared and sequenced from WT, *Dgcr8*$^{-/-}$, and *Dicer*$^{-/-}$ ESCs. Exon-exon boundaries and read numbers from sequencing data are shown (Red). TopHat (http://ccb.jhu.edu/software/tophat/index.shtml) was used for the analysis.

(E) Schematic representation of the mouse miR-17∼92 locus. P1, P2, P3, and P4 indicate the probes used for northern blots in (F). RP1 and RP2 indicate the position of the primers used for the 5′ RACE experiments presented in (G). Sequence of exon 3 (shaded gray) includes the position of the cleavage site identified by 5′ RACE (green font) and the miR-17-5p sequence (red font).

(legend continued on next page)

Moreover, while expression of miR-19, promotes lymphoma in mouse, co-expression of miR-92 suppresses this oncogenic activity (Olive et al., 2013). The miR-19:miR-92 expression ratio in Myc-induced mouse tumors appears to be dynamically regulated during lymphoma progression (Olive et al., 2013). Similarly, whereas ectopic expression of the entire miR-17∼92 cluster can result in the expansion of apparently normal multipotent hematopoietic progenitors, the imbalanced expression of miR-19 or miR-92 results in B cell hyperplasia and erythroleukemia, respectively (Li et al., 2012). Co-expression of miR-17 suppressed the miR-92 oncogenic effects in this context. Consistent with these mouse models, elevated miR-92 and decreased miR-17 expression was observed in B cell chronic lymphocytic leukemia patients with an aggressive clinical phenotype (Li et al., 2012). Taken together, the precise regulation of this miRNA cluster, and importantly, the relative expression of individual miRNAs from within this cluster are critical for development and disease yet the mechanisms that control miR-17∼92 biogenesis remain largely unknown (Guil and Cáceres, 2007; O'Donnell et al., 2005).

Here, we find expression of individual miRNAs from pri-miR-17∼92 to be dynamically regulated during embryonic stem cell (ESC) differentiation. We describe a new paradigm for miRNA regulation in which certain sequences (repression domains) within the pri-miR-17∼92 are involved in the formation of a higher-order RNA conformation that selectively inhibits Microprocessor-mediated production of pre-miR-17, pre-miR-18a, pre-miR-19a, pre-miR-20a, and pre-miR-19b, from this cluster. Cleavage of pri-miR-17∼92 to remove the autoinhibitory 5′ fragment produces a miRNA biogenesis intermediate that we termed "progenitor-miRNA" (pro-miRNA). Pro-miRNA biogenesis is dynamically regulated and specifically requires the endonuclease component of the cleavage and polyadenylation specificity factor complex, CPSF3 (also known as CPSF73 or CPSF-73) (Mandel et al., 2006), as well as the poorly characterized spliceosome factor ISY1. These factors are selectively required for the expression of all miRNAs within the cluster except for miR-92. Thus, developmentally regulated generation of pro-miRNA explains the posttranscriptional control of miR-17∼92 expression. Our findings challenge the current two-step processing model for miRNA biogenesis and add an additional processing step upstream of Microprocessor that can be dynamically regulated for precise miRNA control.

RESULTS

miR-17∼92 Expression Is Regulated Posttranscriptionally during ESC Differentiation

To investigate possible miR-17∼92 regulatory mechanisms, we analyzed miRNA expression during ESC differentiation. As a control we monitored levels of let-7 miRNA that accumulates during the later stages of cell differentiation (Viswanathan et al., 2008). While miR-92 expression was relatively constant throughout the differentiation time course and correlated quite well with expression of pri-miR-17∼92, the relative expression of the other miRNAs from this locus was more dynamic with a peak in miR-17, miR-18a, miR-19a, miR-20a, and miR-19b levels observed around days 2–3 of differentiation (Figures 1A and 1B). Analysis of our small RNA cloning and high-throughput cDNA sequencing data from ESCs revealed a strong predominance of miR-92 sequences compared to other miRNAs in this cluster (Figure 1C). As a first step to investigate the possible mechanisms for this developmentally regulated, posttranscriptional control of miR-17∼92, we performed RNA cloning and high-throughput cDNA sequencing from ESCs to define the pri-miRNA. Since most pri-miRNAs are present at very low levels in steady state RNA, we included Dgcr8 (and Dicer) knockout ESCs in this analysis. The sequencing data from Dgcr8 knockout ESCs indicated that the mouse pri-miR-17∼92 gene spans more than 5 kb and contains multiple introns. The miRNA sequences themselves are located within Intron 3 of the host transcript, similar to the annotated human gene (Figures 1D and 1E). Increased read abundance extended across the entire cluster in Dgcr8 knockout compared to the wild-type cells suggesting that this region contains the Microprocessor substrate RNA that is stabilized in Dgcr8-deficient cells. We also detected an increased number of reads mapping downstream of the miRNA cluster in the Dicer knockout ESCs. This polyadenylated 3′ RNA fragment likely represents a product of Microprocessor-mediated cleavage of pre-miR-92. The elevated abundance of this 3′ RNA fragment in Dicer knockout cells was confirmed by quantitative RT-PCR (qRT-PCR) (data not shown) and is consistent with a feedback mechanism leading to increased pri-miR-17∼92 expression in the absence of the functional mature miRNAs. Altogether, these results reveal that miR-17∼92 miRNAs are embedded in a long, spliced, polyadenylated pri-miRNA expressed from a locus of >5 kb, and the processing and/or stability of the mature miRNAs expressed from this cluster can be dynamically regulated.

Identification of a Processed Pri-miR-17∼92 Intermediate

To validate pri-miRNA sequencing data, we performed northern blots with probes spanning the locus (Figure 1E). We included total RNA, as well as RNA separated into the PolyA(+) and PolyA(−) fractions prepared from wild-type, Dgcr8-, and Dicer-knockout mESCs. A large (>5 kb) transcript was detected in the Dgcr8 knockout RNA samples in both total RNA as well as PolyA(+) RNA with all probes (P1–P4) tested. This likely corresponds to the full-length primary transcript (Figure 1F) and supports the RNA sequencing results. This analysis also identified (with probes P1 and P2) an additional prominent band of ∼2.5 kb that was detected in the total and PolyA(−) RNAs from wild-type and *Dicer*$^{-/-}$ ESCs that corresponds to a 5′ RNA fragment containing Introns 1 and 2 (and likely also Exons 1 and 2). Strikingly, probe 3 (P3), that spans the miRNA sequences in Intron 3, detected a predominant band of ∼800 nt

(F) Northern blots performed on indicated RNAs. Probes are indicated (left) and the schematic (right) represents an interpretation of the northern blot data.
(G) 5′ RACE data from *Dicer*$^{-/-}$ ESCs using the indicated primers. Ethidium bromide-stained agarose gel analysis of RACE products (left) and summary of RACE sequencing data (right). The numbers indicate the proportion of all sequences that map to a particular nucleotide. Mature miRNA sequences are highlighted in red, and miR-17-3p and miR-92a-1* are highlighted in blue.

in the total and PolyA- RNAs (Figure 1F). Finally, a probe complementary to sequences in the 3′ region detected ~2.2 kb band only in the total and PolyA(+) RNA and not in the PolyA(−) RNA from *Dicer*$^{-/-}$ cells. Altogether, these results support that the polyadenylated pri-miRNA, detectable in *Dgcr8*$^{-/-}$ cells, is >5 kb, and this pri-miR-17~92 is cleaved into three major fragments: ~2.5 kb 5′ region, ~800 nt region containing miRNA sequences, and ~2.2 kb 3′ region with a PolyA tail.

5′ Rapid amplification of cDNA ends (5′ RACE) using the indicated primers (Figure 1G) revealed that the majority of the 5′ ends of the polyadenylated 3′ region map to the expected Drosha cleavage site for the biogenesis of miR-92a with the remainder of reads corresponding to Drosha cleavage of pre-miR-19b. However, the 5′ cleavage site occurs 9 nt upstream of the miR-17-5p sequence and is inconsistent with the expected Drosha cleavage. Taken together, these results indicate that the pri-miR-17~92 is specifically cleaved close to the pre-miR-17 hairpin by an unknown nuclease to release a 5′ upstream RNA fragment and that Drosha processing of pre-miR-92 generates the 3′ cleavage to liberate a "progenitor-miRNA" (pro-miRNA) intermediate containing miR-17, miR-18a, miR-19a, miR-20a, and miR-19b.

The 5′ Fragment of Pri-miR-17~92 Inhibits Microprocessor Activity

To examine whether the pro-miRNA might represent a miRNA biogenesis intermediate, we tested different RNA substrates in Microprocessor assays. The pri-miRNA sequence used in these experiments corresponds to a genomic DNA sequence beginning at the 5′ end of Exon 2 and ending at the 3′ end of Exon 6 (Figure 1E). The pro-miRNA starts at the 5′ side of pre-miR-17 and ends ~50 nt downstream of the 3′ end of pre-miR-92. The pro-miRNA^{+}5′F and pro-miRNA^{+}3′F include the pro-miRNA with the additional upstream or downstream sequences present in the pri-miRNA, respectively. These in vitro processing assays revealed that pro-miRNA is a preferential Microprocessor substrate compared to pri-miRNA, and the 5′ region of the pri-miR-17~92 inhibits Microprocessor (Figure 2A).

Cleavage of Pri-miR-17~92 to Pro-miRNA Is a Key Step in miRNA Maturation

To explore the functional impact of pro-miRNA biogenesis, we performed rescue experiments in mouse ESCs in which the endogenous miR-17~92 is deleted. *miR-17~92*$^{-/-}$ ESCs were transfected with plasmids expressing either the wild-type pri-miR-17~92 or a mutant version in which two nucleotides (AG) at the potential cleavage site were mutated. qRT-PCR analysis indicated that both plasmids produced similar levels of pri-miRNA (Figure 2B) yet when PCR primers spanning the cleavage site were used a strong accumulation of the uncleaved RNA was detected supporting that the mutation inhibits pri-miRNA cleavage (Figure 2B). Northern blot analysis detected a cleaved 5′ fragment specifically in cells expressing the wild-type plasmid (Figure 2C). We next examined the consequence of this cleavage site mutation on mature miRNA biogenesis. Analysis of miRNA expression by qRT-PCR and by northern blot revealed that the AG-CC mutation inhibits expression all miRNAs in the cluster except for miR-92 (Figure 2D and 2E). Since the plasmid expressing pro-miR-17~92 also contains a small amount of upstream sequence that includes the cleavage site, we could also test the effect of the same AG-CC mutation in this context. The AG-CC mutation had no effect on miRNA biogenesis expressed from the pro-miR-17~92 plasmid (Figures 2D and 2E). Next, to examine whether pro-miRNA biogenesis is an important step for the expression of endogenous miRNAs, we used CRISPR/Cas9 technology to engineer the AG-CC mutation at the pri-miR-17~92 locus in ESCs. Introduction of this mutation led to dramatically diminished expression of miR-17, miR-18a, miR-19a, miR-20a, and miR-19b compared to wild-type cells but had no effect on endogenous miR-92 expression (or an unrelated control miRNA, miR-21) (Figure 2F). These results suggest that the 5′ region of pri-miR-17~92 inhibits production of most miRNAs in this cluster except for miR-92 and that this autoinhibitory mechanism might explain the posttranscriptional regulation of pri-miR-17~92 expression that we observed in ESCs (Figure 1A).

Since the 5′ RACE strategy could not accurately distinguish whether cleavage occurred after the A or the G nucleotides in the pri-miR-17~92 (due to the dCTP 3′ tailing of the cDNA with terminal deoxynucleotidyl transferase and use of complementary oligo-G containing PCR primer), we performed additional mutagenesis at the cleavage site and examined the effects on miRNA expression. This revealed that mutation of the G nucleotide had no impact on miR-17~92 whereas the A mutation (as well as mutation of the preceding C nucleotide) dramatically suppressed miRNA expression comparable to the AG mutant (Figure S1). Together, these results demonstrate that cleavage of the autoinhibitory 5′ RNA fragment to generate pro-miRNA is an obligate step for the biogenesis of miRNAs from the pri-miR-17~92.

Identification of Two Complementary Repression Domains that Control miRNA Biogenesis

To define the *cis*-regulatory RNA sequences present in the 5′ fragment of pri-miR-17~92, additional genetic rescue experiments were performed using a panel of pri-miR-17~92 expression constructs in which portions of the 5′ inhibitory fragment are deleted. This identified a domain ~80–120 nt upstream of the cleavage site responsible for the selective miRNA repression (Figure 3A). This was confirmed by similar experiments in which only the 40 nt repression domain (RD) was deleted in the context of the pro-miR-17~92 containing the 5′ fragment (Figure 3B). To further examine the function of the RD, we performed in vitro Microprocessor assays. To distinguish processing of the individual pre-miRNAs from the cluster, we performed Microprocessor assays using non-radiolabeled substrate RNAs and visualized pre-miRNAs by northern blot. This confirmed that the ~40 nt RD within the 5′ region of pri-miR-17~92 selectively inhibits the processing of pre-miR-17, pre-miR-18, pre-miR-19, and pre-miR-20 from the cluster but has no inhibitory effect on the processing of pre-miR-92 (Figure 3C). Altogether, these results suggest that the RD in the 5′ region of pri-miR-17~92 inhibits production of most miRNAs in this cluster except for miR-92 and that this autoinhibitory mechanism might explain the posttranscriptional regulation of pri-miR-17~92 expression.

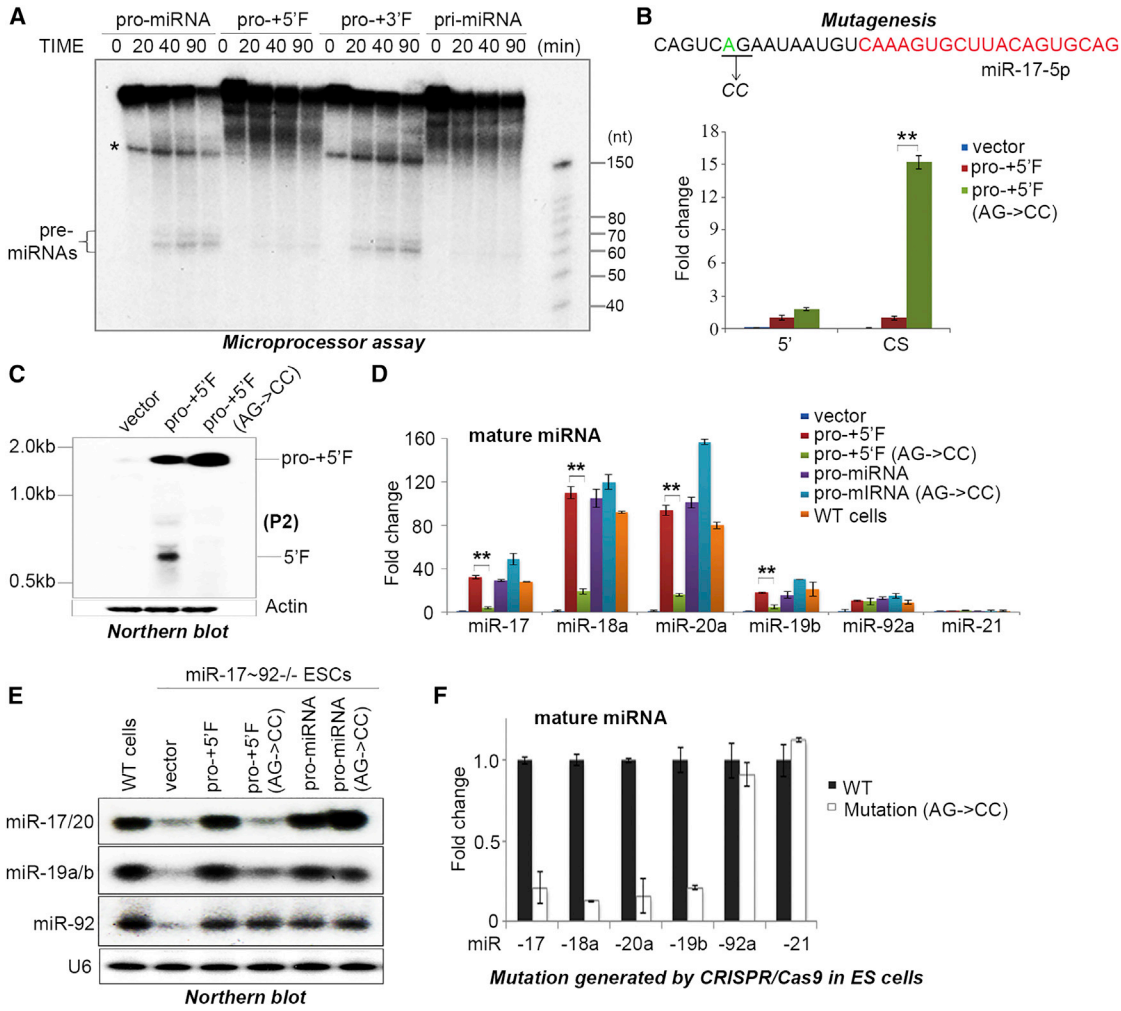

Figure 2. Cleavage of Pri-miR-17∼92 to Pro-miRNA Is a Key Step in miRNA Maturation

(A) Microprocessor cleavage assays performed using the indicated substrates. Asterisk denotes a truncated or non-specific RNA.

(B) qRT-PCR analysis of the relative expression of regions of miR-17∼92 expressed from the indicated plasmids. Primers amplifying the 5′ upstream sequence (5′) and primers spanning the cleavage site (CS) were used to detect pri-miR-17∼92 in transfected *miR-17∼92*$^{-/-}$ ESCs. Data normalized to ACTIN and represented as mean ± SEM. **p < 0.01, Student's t test.

(C) Northern blot analysis of the RNA samples in (B) using a probe that detects the 5′ upstream region of pri-miR-17∼92 (P2).

(D) *miR-17∼92*$^{-/-}$ ESCs were transfected with the indicated rescue plasmids and mature miRNAs measured by qRT-PCR. Data normalized to snoR142 and represented as mean ± SEM. **p < 0.01, Student's t test.

(E) Northern blot analysis of the RNAs from (D) using probes to detect the indicated miRNAs.

(F) qRT-PCR analysis of the indicated endogenous mature miRNAs expression in ESCs engineered with a mutation in the cleavage site at the endogenous pri-miR-17∼92 locus. Data are normalized to snoR142 and represented as mean ± SEM.

See also Figure S1.

We considered that the RD might impact the secondary structure of this pri-miRNA cluster to suppress Microprocessor activity. The secondary structure of pri-miR-17-92 containing the minimal RD was computationally predicted using the RNAFold algorithm (http://rna.tbi.univie.ac.at/cgi-bin/RNAfold.cgi). This indicated that the RD might base-pair with a highly conserved sequence that we termed repression domain* (RD*) that is located between pre-miR-19b and pre-miR-92 (Figures 3D, 3E, and S2). We found this intriguing since this complementary RD* is located at the boundary of the miRNAs whose processing is suppressed miR-92 that escapes repression. The ability of RD and RD* sequences to form a duplex was experimentally confirmed (Figure 3E), and genetic rescue experiments with plasmids lacking the RD* revealed the requirement of this region for miRNA repression (Figures 3B and 3F). Deletion of the RD or the RD* had a similar effect on Microprocessor activity indicating that both domains are important for the autoinhibition of miRNA biogenesis (Figure 3G). To test the model that base-paring between the RD and RD* is important for miRNA regulation, we generated expression plasmids with either the RD or RD* mutated. Individual RD or RD* mutations led to elevated miRNA expression, whereas combining the compensatory mutations

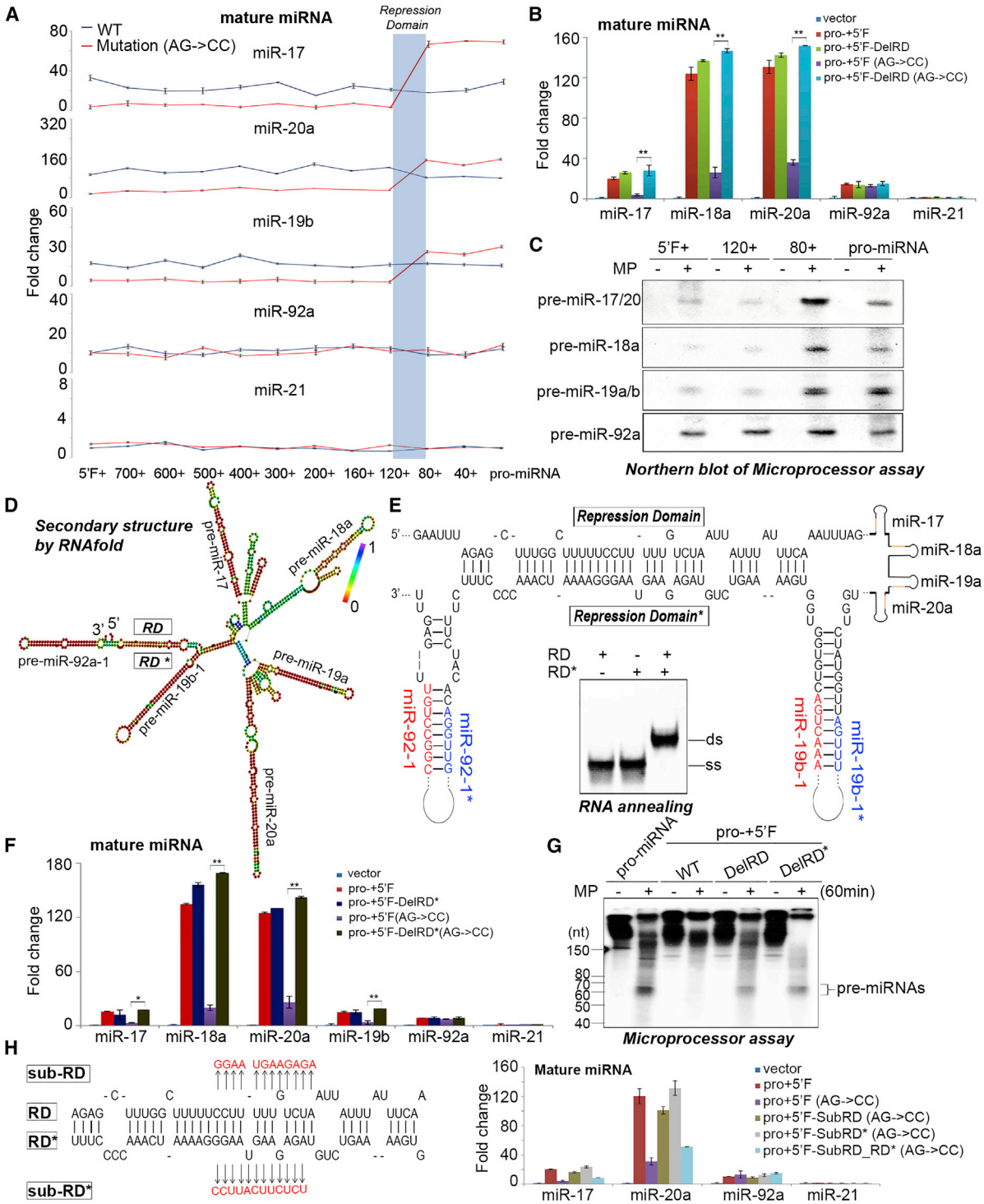

Figure 3. Identification of Two Complementary Repression Domains Controlling miRNA Biogenesis

(A and B) Genetic rescue experiments in which *miR-17∼92*$^{-/-}$ ESCs were transfected with the indicated rescue plasmids and mature miRNAs measured by qRT-PCR. The ∼40 nt repression domain (RD) is highlighted with blue shading in (A). Data normalized to snoR142 and represented as mean ± SEM. **p < 0.01, Student's t test.

(C) In vitro Microprocessor assays with non-radiolabeled substrate RNAs. Aliquots of the reaction were loaded onto multiple gels, transferred to nylon membranes, and individual pre-miRNAs detected by northern blot using the indicated probes.

(D) Secondary structure prediction of the minimal pri-miRNA fragment containing the 5′ repression domain (RD) using the RNAFold algorithm (http://rna.tbi.univie.ac.at/cgi-bin/RNAfold.cgi). The region (termed RD*) that is complementary to the RD is depicted. RD*, repression domain star.

(legend continued on next page)

that restored base-pairing between RD and RD* reestablished miRNA repression (Figure 3H).

Pri-miR-17∼92 Adopts an RNA Conformation that Inhibits Microprocessor

To gain insight into the mechanism by which pri-miR-17∼92 processing might be regulated, we tested the possible involvement of RNA conformational changes mediated by the RD and RD*. The extent to which Microprocessor was selectively inhibited was found to be sensitive to RNA annealing in the presence of $MgCl_2$—a result that further implicated RNA conformation in miRNA repression (Figure 4A). We next analyzed the differential RNase T1 accessibility of pro-miR-17∼92 with or without the 5′ fragment. This revealed that the 5′ fragment confers striking resistance to nuclease digestion, further supporting that the pro-miR-17∼92 containing the 5′ fragment adopts a compacted conformation (Figure 4B). To gain direct evidence that the pri-miRNA containing the 5′ RD adopts a distinct conformation, we used electron microscopy to directly visualize the higher order structure of different RNAs. This analysis revealed that a pri-miR-17∼92 fragment containing both the RD and RD* forms highly compacted, circular particles ∼12 nM in diameter whereas RNAs lacking either the RD or the RD* did not form particles under the same conditions (Figures 4C and 4D). Altogether, these results uncover an important role for the RD and the RD* in the dynamic control of pri-miR-17∼92 biogenesis through the formation of a compacted RNA conformation that is refractory to cleavage by Microprocessor.

CPSF3 Endonuclease Is Required for Pro-miRNA Biogenesis and miRNA Expression

To identify protein factors that might be involved in pro-miRNA biogenesis and the posttranscriptional regulation of miR-17∼92 expression, we performed RNA affinity purification using both pri-miR-17∼92 and pro-miR-17∼92 RNA sequences and identified associated proteins by mass spectrometry. Several RNA-binding proteins including DGCR8 were identified in both RNA purifications, whereas other proteins were found exclusively in the pri-miR-17∼92 purification—the majority of which fall into two main categories, factors involved in pre-mRNA 3′ end cleavage and splicing regulators (Figure 5A). Since the cleavage and polyadenylation specificity factor (CPSF) complex possesses ribonuclease activity, we initially focused on the possible role of components of this complex in miR-17∼92 biogenesis. We used siRNAs to knockdown CPSF2 (also known as CPSF-100), CPSF3 (also known as CPSF-73), CSTF2 (CstF-64), CSTF2T (TCstF-64), or FIP1L1 in ESCs and examined the effects on mature miRNA expression. We found CPSF3, but not CPSF2 or other mRNA cleavage/polyadenylation factors tested, is specifically required for expression of all the miRNAs in the cluster except for miR-92 (Figures 5B–5D and S3). As a positive control, DGCR8-depletion decreased expression of all miRNA tested. Moreover, northern blot analysis revealed that CPSF3 (but not CPSF2) is required for pro-miR-17∼92 biogenesis (Figure 5E). These experiments were performed in *Dicer*$^{-/-}$ ESCs since the level of pri-miR-17∼92 is elevated in these cells. Genetic rescue of *miR-17∼92*$^{-/-}$ ESCs with miRNA expression plasmids revealed that CPSF3 is specifically required for miRNA expression from the pri-miRNA containing the 5′ region and not from the pro-miRNA (Figure 5F). Considering the established role of CPSF3 as the endonuclease responsible for the cleavage of the 3′ end of both pre-mRNA and histone mRNA, as well as the known CPSF3-mediated cleavage at "CA" dinucleotides, we hypothesized that CPSF3 might be the endonuclease that cleaves pri-miRNA-17∼92 to remove the RD and license Microprocessor activity (Dominski et al., 2005; Mandel et al., 2006). To directly test this, we generated recombinant CPSF3 (rCPSF3) and a catalytic mutant (D75K/H76A) version of CPSF3 purified from *Escherichia coli* and performed in vitro cleavage assays using different RNA substrates. We found that a fragment of pri-miR-17∼92 containing the 5′ repression domain, cleavage site, and the entire pre-miR-17 sequence is specifically cleaved by rCPSF3, whereas a slightly truncated RNA that lacks the pre-miR-17 stem loop was not an efficient substrate (Figures 5G and 5H). Mutation (AG-CC) at the cleavage site abolished CPSF3-mediated pri-miRNA cleavage, and the catalytic mutant CPSF3 was inactive in these assays (Figure 5I). We furthermore found that addition of rCPSF3 to Microprocessor assays could relieve the inhibition mediated by the 5′ fragment of pri-miR-17∼92 (Figure 5J). Altogether, these data strongly support our model that CPSF3 is the nuclease responsible for specific pri-miRNA cleavage to remove the repression domain and license Microprocessor-mediated production of pre-miRNA from this cluster.

Spliceosome Subunits Are Required for Pro-miRNA Biogenesis and miRNA Expression

Considering our mass spectrometry data as well as a previous report that found that processing the 3′ end of histone pre-mRNAs by CPSF3 requires components of the U7 snRNP we next examined whether certain spliceosome subunits might help recruit the CPSF3 endonuclease activity to pri-miR-17∼92 in vivo (Dominski et al., 2005). We initially focused on ISY1, a poorly characterized homolog of the non-essential Isy1p protein in yeast. Isy1p is a subunit of the NineTeen Complex and is involved in the first step of splicing to control splicing fidelity (Dix et al., 1999; Villa and Guthrie, 2005). We added to our characterization, SF3B1, a component of the U2 small nuclear ribonucleoprotein complex (U2 snRNP) that although not identified

(E) A zoomed-in view of the base-pairing between RD and RD*. Inset shows the in vitro annealing and native PAGE analysis of synthetic RD and RD* RNA sequences.

(F) Genetic rescue with the indicated plasmids and mature miRNAs measured by qRT-PCR. Data are normalized to snoR142 and represented as mean ± SEM. *$p < 0.05$, **$p < 0.01$, Student's t test.

(G) Microprocessor cleavage assays.

(H) As in (B) and (F) but using plasmids with the indicated nucleotide substitutions (red font).

See also Figure S2.

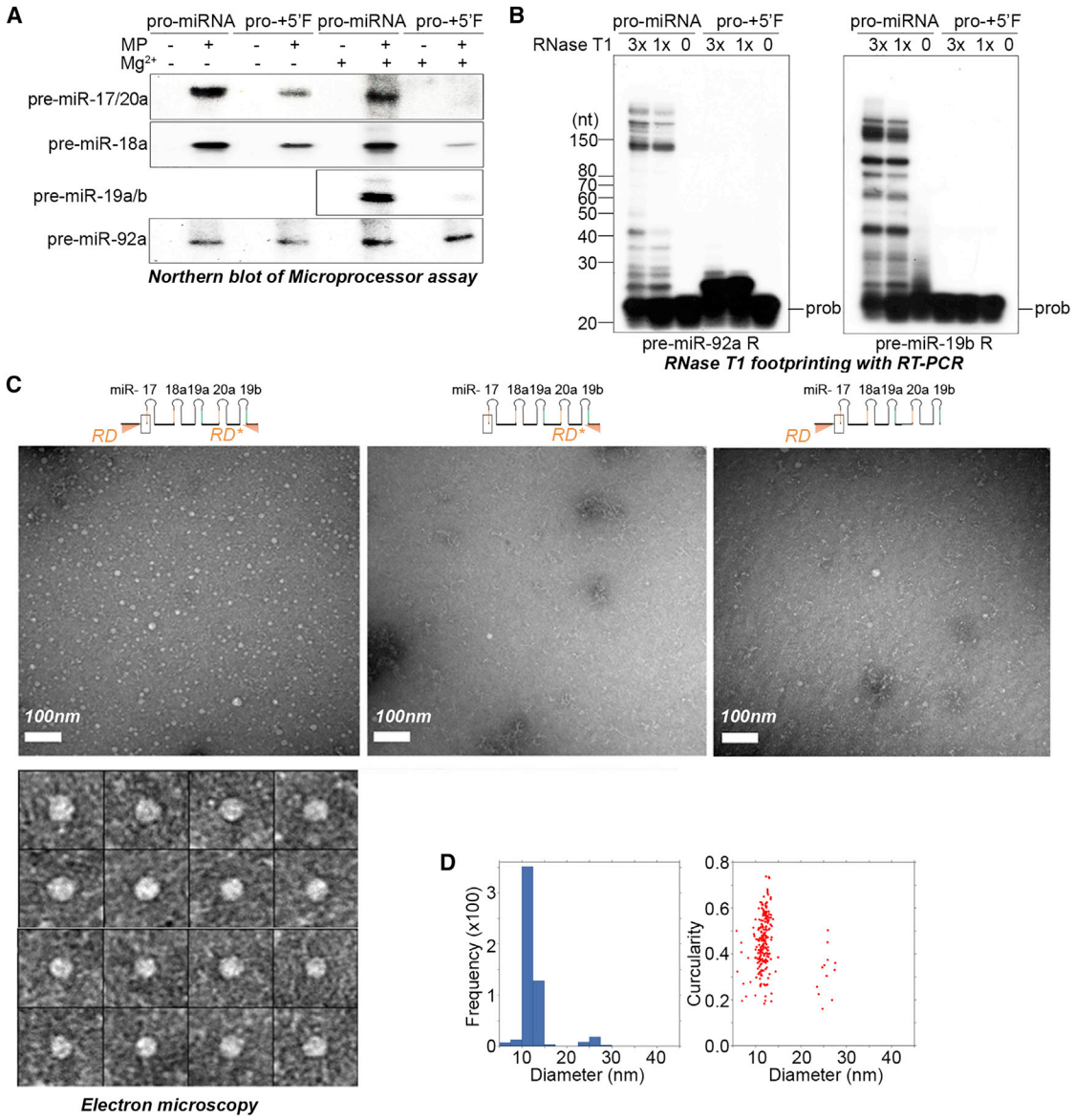

Figure 4. Pri-miR-17∼92 Adopts an RNA Conformation that Inhibits Microprocessor

(A) Microprocessor cleavage assays performed with (+) or without (–) RNA annealing in the presence of $MgCl_2$. Reaction products were loaded onto multiple gels and analyzed by northern blot.

(B) RNase T1 accessibility assays performed using the indicated RNA and analyzed by reverse transcriptase primer extension using the indicated 5′-end-labeled primers.

(C) Negative-stain micrographs of indicated RNAs in the presence of $MgCl_2$. Specimens were prepared in uranyl acetate. Lower panel shows representative images of RD-Pro-RD* particles.

(D) 2D distribution of RD-Pro-RD* particles based on their diameter and circularities.

in our mass spectrometric analysis of pri-miR-17∼92-associated proteins is a much more well characterized splicing factor. We used siRNAs to individually knockdown ISY1 and SF3B1 in ESCs and examined the effects on miRNA expression (Figures 6A–6C). This revealed that depletion of ISY1 or SF3B1 led to diminished expression of all miRNAs in the pri-miR-17∼92 cluster with the exception of miR-92 and a corresponding accumulation of pri-miR-17∼92 (Figure 6B). Northern blots confirmed the role of these splicing factors in pro-miRNA biogenesis (Figure 6D). RNAi knockdown of multiple additional spliceosomal factors revealed a specific requirement for ISY1 as well as U2 snRNP components (SF3B1 and U2AF2) but not other splicing factors associated with the second step of splicing including PRPF4 (U4/U6 snRNP), SNRNP40 (U5 snRNP (Figure S4). These findings help clarify the requirement of certain splicing factors and strongly support our model that ISY1 together with ISY1

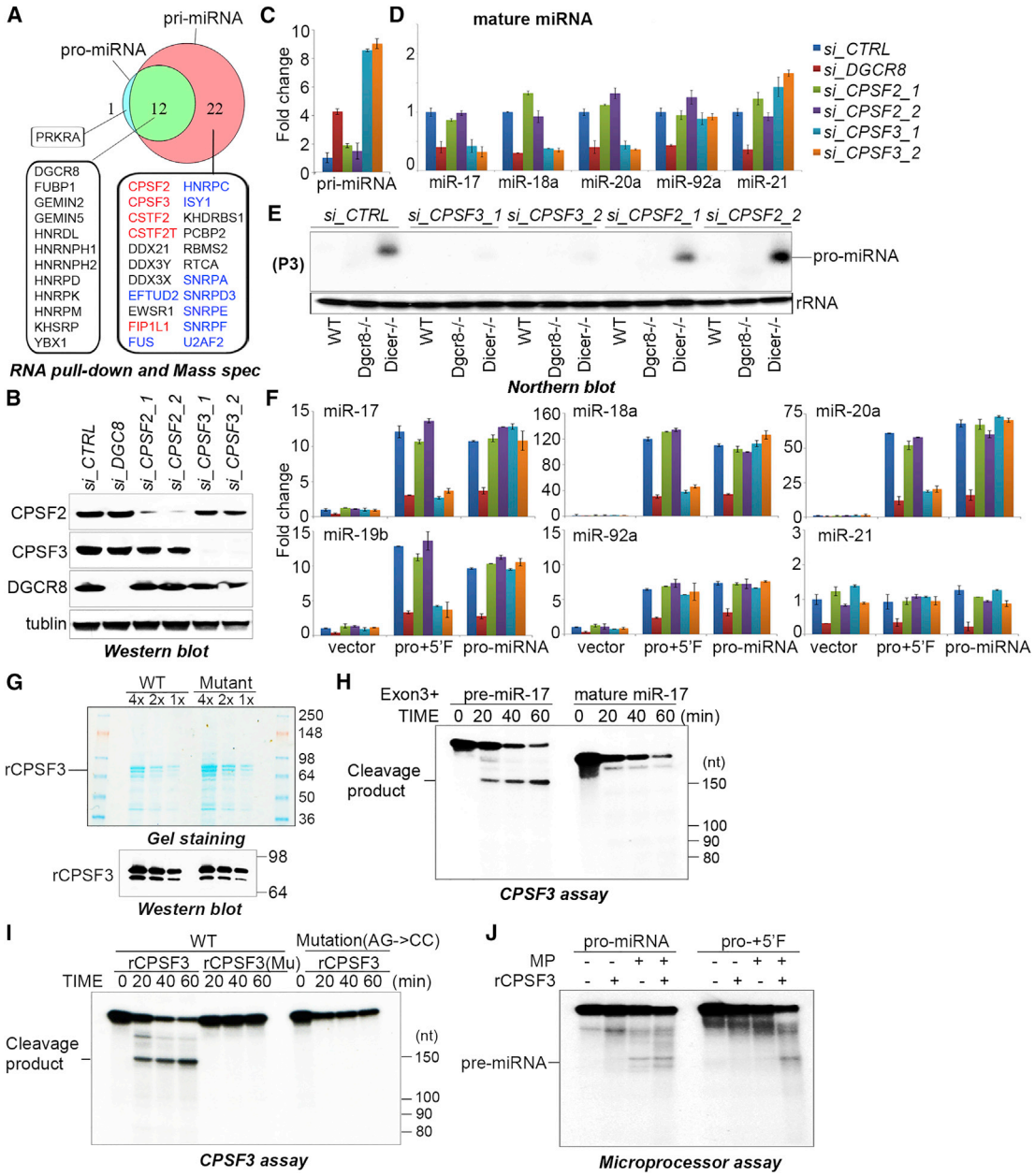

Figure 5. CPSF3 Endonuclease Is Required for Pro-miRNA Biogenesis and Mature miRNA Expression

(A) Summary of mass spectrometric analysis of RNA-affinity purifications. Factors known to be involved in pre-mRNA 3′ cleavage and polyadenylation are highlighted in red and proteins involved in splicing are listed in blue.

(B) Western blot of lysates prepared from ESCs transfected with the siRNAs and analyzed using the indicated antibodies.

(C) qRT-PCR analysis of pri-miRNA expression in cells with indicated siRNA knockdown. Data normalized to ACTIN and represented as mean ± SEM.

(D) qRT-PCR analysis of the indicated endogenous miRNAs in ESCs transfected with the siRNAs shown. Data normalized to snoR142 and represented as mean ± SEM.

(E) Northern blot performed on total RNA, from WT, *Dgcr8*$^{-/-}$, and *Dicer*$^{-/-}$ ESCs transfected with the indicated siRNAs. A probe was used to detect pro-miRNA as indicated on the right (P3).

(F) qRT-PCR analysis of the relative expression the indicated miRNAs expressed from the indicated miR-17∼92 rescue plasmids co-transfected with the indicated siRNAs. Data normalized to snoR142 and represented as mean ± SEM.

(G) Coomassie blue stained SDS-PAGE gel (top) and αCPSF3 western analysis (bottom) of recombinant His-CPSF3 purified from *E. coli*. Wild-type (WT) and a catalytic mutant CPSF3 (D75K/H76A) were produced.

(H and I) CPSF cleavage assays using the indicated in vitro transcribed RNA substrate and His-CPSF3 (WT or Mutant).

(J) Microprocessor cleavage assay with the indicated RNA substrate and with addition of His-CPSF3 where indicated.

See also Figure S3.

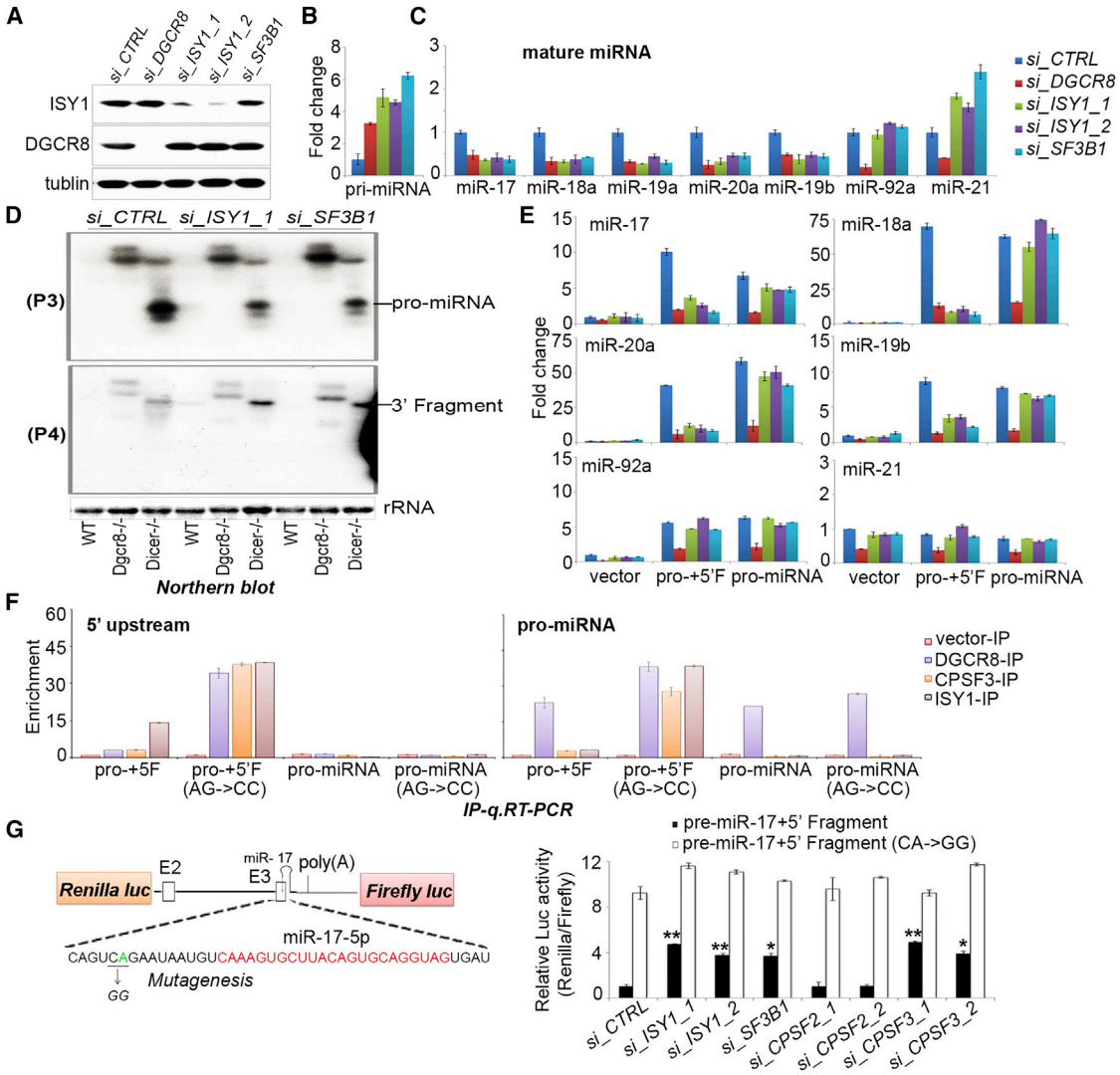

Figure 6. Spliceosome Subunits Are Required for Pro-miRNA Biogenesis and miRNA Expression

(A) Western blot of lysates prepared from ESCs transfected with the siRNAs and analyzed using the indicated antibodies.

(B) qRT-PCR analysis of pri-miRNA expression in cells with indicated siRNA knockdown. Data are normalized to ACTIN and represented as mean ± SEM.

(C) qRT-PCR analysis of the indicated endogenous miRNAs in ESCs transfected with the siRNAs shown. Data are normalized to snoR142 and represented as mean ± SEM.

(D) Northern blots performed on indicated RNAs.

(E) qRT-PCR analysis of the relative expression the indicated miRNAs expressed from the indicated *miR-17∼92*$^{-/-}$ rescue plasmids. Data are normalized to snoR142 and represented as mean ± SEM.

(F) Flag immunoprecipitation (Flag-IP) assays performed from cells expressing the indicated Flag-tagged cDNAs together the indicated miRNA expressing plasmids. qRT-PCR was performed on RNAs collected from the purified complexes and the relative enrichment of the pro-miRNA signal in the IP compared with input samples is plotted for each protein.

(G) Schematic representation of the WT and the cleavage mutant luciferase reporters (top). Reporter assays in 293 cells were performed in triplicate and the indicated siRNAs were co-transfected with the reporter plasmid DNA (bottom). *p < 0.05, **p < 0.01, versus control sample, Student's t test.

See also Figure S4.

and the U2 snRNP are specifically required for pro-miRNA biogenesis.

To provide more evidence that splicing factors are selectively required for miR-17∼92 expression, we performed rescue experiments in miR-17∼92 knockout ESCs. We found that whereas DGCR8 was required for expression of miRNAs from both the pro-miR-17∼92 as well as the plasmid containing pro-miR-17∼92 with the upstream sequences (pro+5′F), the splicing factors ISY1 and SF3B1 were specifically required for the expression of miRNAs from pro+5′F (Figure 6E).

To further confirm the role of these factors in pro-miRNA biogenesis, we affinity-purified DGCR8, CPSF3, and ISY1 containing ribonucleoprotein complexes from cells and analyzed the associated RNA by qRT-PCR. For these experiments, cells

were co-transfected with plasmids expressing the indicated Flag-tagged protein together with plasmids expressing either wild-type pri-miR-17∼92, the cleavage site mutant version of pri-miR-17∼92, or the corresponding pro-miRNAs. This revealed that unlike DGCR8 that associates with all the RNAs tested, CPSF3 and ISY1 specifically associate with the cleavage site mutant pri-miR-17∼92, consistent with the specific role of these factors in pro-miRNA biogenesis (Figure 6F).

A Luciferase reporter containing the 5′ region of pri-miR-17∼92 was generated. Pri-miR-17∼92 sequences (beginning from the start of exon 2 and ending in the pre-miR-17 hairpin) were cloned into the 3′ UTR of the Renilla luciferase gene (Figure 6G). We previously used a similar approach to monitor Microprocessor activity (Mori et al., 2014). We used this reporter and a reporter containing a mutated cleavage site to examine the effects of ISY1, SF3B1, CPSF2, and CPSF3 knockdown on the relative luciferase values. For factors involved in cleavage of the 5′ region of pri-miR-17∼92, we expect to see a stabilization of the Renilla luciferase relative to a control Firefly luciferase upon knockdown. We found that depletion of ISY1, SF3B1, and CPSF3, but not CPSF2, led to increased Renilla relative to Firefly luciferase. Importantly, this effect was specific to the wild-type pri-miR-17∼92 fragment since depletion of these same factors had no stabilizing effect on the cleavage site mutant reporter. Taken together, our data support that spliceosome components and the CPSF3 endonuclease subunit of the pre-mRNA 3′ processing complex, are specifically required for cleavage of the pri-miRNA.

Pro-miRNA Biogenesis Controls miR-17∼92 Expression in Embryonic Stem Cells

We considered that developmentally regulated expression of some of these factors required for pri-miR-17∼92 processing might be responsible for the dynamic miRNA expression during ESC differentiation (Figures 1A and 1B). We measured the relative gene expression during ESC differentiation and found ISY1 expression level to be correlated with miRNA expression with a peak at day 3 of ESC differentiation (Figures 7A and 7B). Furthermore, ISY1 expression also correlated with cleavage of the 5′ region of pri-miR-17∼92 since primers spanning the cleavage site (but not other regions of pri-miR-17∼92) showed a decline in signal by qRT-PCR at day 3 (Figure 7C). These correlative data suggested that ISY1 might be a limiting factor in ESCs for the processing of certain miRNAs from pri-miR-17∼92. To test this, we overexpressed ISY1 in ESCs and measured the effects on miRNA expression. We found that ISY1 overexpression in this context caused a selective miRNA upregulation and corresponding increase in cleaved pri-miR-17∼92 (Figure 7D). These results indicate that the developmentally regulated generation of pro-miRNA is likely responsible for the posttranscriptional control of miR-17∼92 expression in ESCs.

Considering the developmental requirement of ISY1 for miRNA expression and the involvement of both ISY1 and CPSF3 in pro-miRNA biogenesis, we next examined the possible physical and functional interaction between ISY1, CPSF3, and the Microprocessor. ISY1 and CPSF3 were found to specifically associate with Drosha and DGCR8 in co-immunoprecipitation (coIP) experiments (Figures 7E and 7F). Whereas this interaction with Microprocessor was strongly diminished by RNase treatment, the interaction between ISY1 and CPSF3 complexes is likely not mediated by RNA (Figure 7F). Functionally, we found that addition of immunopurified Flag-ISY1 complex could enhance the specific CPSF3-catalyzed pri-miRNA cleavage in vitro (Figure 7G).

DISCUSSION

Here, we uncover a new paradigm for miRNA expression control. While proteins that inhibit or promote the biogenesis of certain miRNAs are known, our discovery that *cis*-acting sequences within a pri-miRNA can selectively and dynamically regulate expression of a miRNA cluster through the formation of an inhibitory RNA conformation reveals an additional posttranscriptional mechanism for the precise control of miRNA expression. This mechanism also allows the uncoupling of expression of individual miRNAs from within a single pri-miRNA cluster. In exploring the mechanism of the dynamic posttranscriptional control of pri-miR-17∼92 miRNA expression during ESC differentiation, we identified a miRNA biogenesis intermediate that we termed progenitor miRNA (pro-miRNA). Specific cleavage of an autoinhibitory 5′ RNA fragment is required to selectively license Microprocessor-mediated production of most pre-miRNAs from pri-miR-17∼92. We employed a biochemical approach to identify possible factors involved in pro-miRNA biogenesis and showed, using a variety of approaches, that the CPSF3 ribonuclease as well as the spicing factor ISY1 (and other U2 snRNP components) are required for pro-miRNA biogenesis and selective expression of all miRNAs within the cluster except for miR-92. We find that developmentally regulated ISY1 expression is critical for controlling expression of miRNAs from pri-miR-17∼92 during ESC differentiation.

Our identification of pro-miRNA upstream of Microprocessor challenges the current two-step processing model for miRNA biogenesis and adds an additional regulatory step for the posttranscriptional control of miR-17∼92 expression. It will be interesting to explore the more widespread relevance of pro-miRNA intermediates in the miRNA biogenesis pathway. In this regard, large, partially processed, pri-miRNAs have been observed in mouse ESCs (Houbaviy et al., 2005). Our identification of two complementary repression domains that nucleate the formation of a repressive higher order RNA conformation to control miRNA biogenesis might also be a relevant mechanism for the control of other RNAs including protein-coding mRNAs. Our results also highlight a potential limitation of in vitro Microprocessor assays that typically utilize artificially truncated "pri-miRNAs" substrates and therefore might miss important regulatory mechanisms that exist in cells.

Our data implicate RNA conformation in the selective inhibition of Microprocessor cleavage of pri-miR-17∼92. A role for RNA tertiary structure in regulating miR-17∼92 has been previously suggested (Chakraborty et al., 2012; Chaulk et al., 2011, 2014). However, those reports deal exclusively with the miR-17∼92 cluster without any flanking sequences (i.e., the equivalent of the pro-miRNA). Also, the proposed model whereby the miR-17∼92 cluster adopts a globular tertiary structure with pre-miR-19b and pre-miR-92 at the core does not correlate well

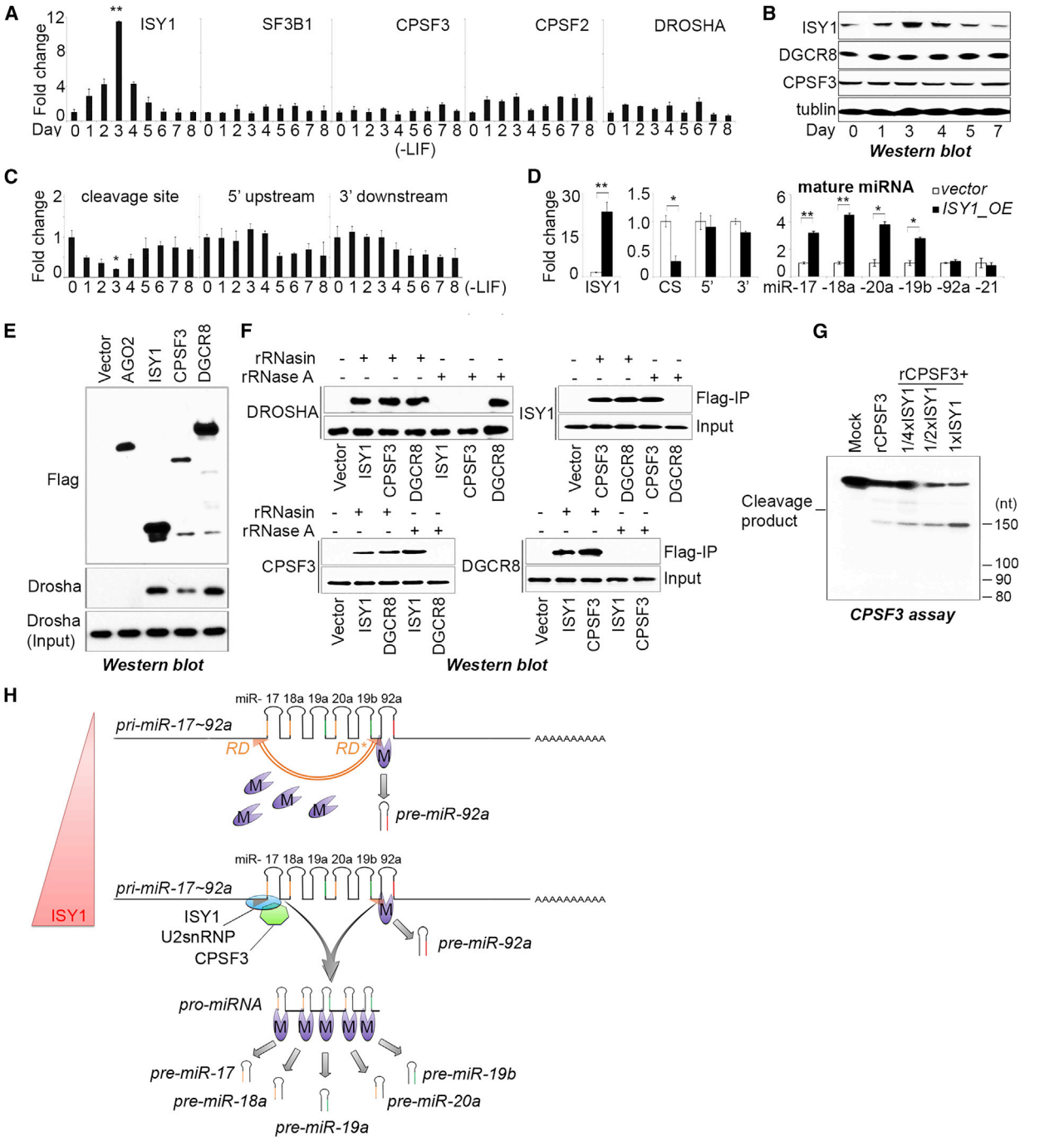

Figure 7. Pro-miRNA Biogenesis Controls miR-17∼92 Expression in Embryonic Stem Cells

(A) qRT-PCR analysis of the indicated mRNA over a differentiation time course. Data are normalized to ACTIN and represented as mean ± SEM. **p < 0.01, Student's t test.

(B) Western blot analysis.

(C) qRT-PCR analysis of the relative expression of regions of the endogenous pri-miR-17∼92 during ESC differentiation. Primers amplifying a region spanning the cleavage site (CS), a region in the 5′ upstream sequence (5′), and a region in the 3′ downstream sequence (3′) of pri-miR-17∼92 were used. Data are normalized to ACTIN and represented as mean ± SEM. *p < 0.05, Student's t test.

(D) qRT-PCR analysis of ectopic ISY1 expression, endogenous pri-miR-17∼92 expression using the primers as in (C) and the endogenous miRNAs indicated. Data are normalized to sno142 (for miRNAs) and ACTIN (for pri-miRNA) and represented as mean ± SEM. *p < 0.05, **p < 0.01, Student's t test.

(legend continued on next page)

with the relative abundance of mature miRNAs in cells since miR-19b, and/or miR-92 are often the most highly expressed members of the cluster. The physiological relevance of this work therefore remains unclear (Chaulk et al., 2011).

The exact mechanism and full repertoire of factors responsible for the coupling of pri-miR-17∼92 transcription, recruitment of CPSF3, ISY1, and other spliceosome subunits for the precise cleavage of the autoinhibitory RNA fragment, and subsequent processing by Microprocessor remain active areas of investigation. CPSF3 is known to be required for the cleavage of mRNAs and is also involved in the generation of the 3′ end of (non-polyadenylated) histone mRNAs (Dominski et al., 2005; Mandel et al., 2006). In the latter case, CPSF3 cleavage activity is directed by the U7 small nuclear ribonucleoprotein (snRNP) (Dominski et al., 2005). We find that although CPSF3 protein is sufficient to specifically cleave pri-miR-17∼92 in vitro, this activity is enhanced by ISY1 complex, and ISY1 is required for pro-miRNA biogenesis in cells. The physical association of CPSF3 with both the U1 SnRNP as well as the U2 snRNP has been reported (Kyburz et al., 2006; Wassarman and Steitz, 1993). We find a role for components of the U2 snRNP, and in particular, a poorly characterized protein ISY1 that likely helps recruit and direct CPSF3 activity. Furthermore pri-miR-17∼92 cleavage does not lead to polyadenylation since the 5′ fragment is detected specifically in the polyA- RNA fraction suggesting that these activities are uncoupled in this context. Drosha is known to physically associate with the spliceosome yet the precise functional relevance of this interaction is not completely understood and might be variable depending on the particular pri-miRNAs (Kataoka et al., 2009; Kim and Kim, 2007; Morlando et al., 2008; Pawlicki and Steitz, 2010). Our model implicates multiple protein complexes and different activities that converge to regulate pro-miRNA biogenesis in a developmentally regulated manner (Figure 7H).

This work examined the developmental regulation of miR-17∼92 expression. Considering the strong links of this miRNA cluster with numerous human malignancies it will be of great interest to further explore the relevance of this control mechanism in the context of cancer.

EXPERIMENTAL PROCEDURES

Cell Culture, ESC Differentiation, and Transfection

ESCs were cultured in DMEM with ESGRO (1,000 units/ml), with 15% (v/v) FBS and antibiotics. For ESC differentiation, ESGRO was removed from the media and cells collected daily. HEK293 cells were cultured in DMEM with 15% (v/v) FBS (Gregory et al., 2004). Lipofectamine 2000 (Invitrogen) was used for all transfections.

Plasmids and Site-Directed Mutagenesis

cDNA of mouse pri-miR-17∼92 was cloned into EcoRI and XhoI sites of pcDNA3 (Invitrogen) and as XhoI and NotI sites of psiCHECK-2 (Promega). cDNAs of mouse ISY1 and CPSF3 were cloned into BamHI and SalI sites of pFlag-CMV2 (Sigma) and CPSF3 cDNA was subcloned into SalI and NotI sites of pETDuet-1 Vector (Novagen). pFlag-CMV2-DGCR8 plasmid was described (Gregory et al., 2004). Primers used for CRISPR/Cas9 mutagenesis were designed (http://crispr.mit.edu/) and cloned into PX330 vector. Q5 Site-Directed Mutagenesis Kit (NEB) was used for mutagenesis. All cloning primers are listed in Table S2.

RNA Purification and Northern Blots

Total RNA was extracted using Trizol (Invitrogen). Total RNA (200 μg) was used for polyA(+) RNA isolation with the Dynabeads mRNA Purification Kit (Invitrogen) following the manufacturer' s instructions, while the supernatant in the step of the binding of oligo(dT) cellulose was kept and an equal volume of isopropanol added to precipitate PolyA(−) RNA. PolyA(+) (200 ng), 20 μg polyA(−), and 20 μg total RNA were loaded on 15% formaldehyde-agarose gels for large RNA northern blot. The cDNAs amplified by PCR corresponding to the different regions of mouse pri-miR-17∼92 were labeled by ^{32}P-dCTP using DNA Polymerase I, Large (Klenow) Fragment (NEB) and used as probes. Small RNA northern blot was performed as described (Gregory et al., 2004). Probes and primers are listed in Table S3.

RNA Cloning and Sequencing

PolyA(+) (200 ng) RNA isolated as described above was used for mRNA-seq. Sample preparation was with the TruSeq Stranded mRNA Sample Prep Kits (Illumina). Small RNA-seq sample preparation was performed as previously described (Thornton et al., 2014). Both sets of samples were subjected to Illumina high-throughput sequencing. For the analysis of mRNA-seq data, TopHat software was used. Bowtie software was used for the alignment of small RNAs to mature miRNA sequences (http://www.mirbase.org/) without any mismatches permitted.

5′ RACE

5′ RACE was performed on 50 ng PolyA(+) RNA and 5 μg PolyA(−) RNA using the 5′ RACE System (Invitrogen). Gene-specific primers were used for reverse transcription and then cDNAs were purified and a dC-tail added using TDT. Two rounds of PCR were performed and the amplicons were cloned into pGEM-T Easy vector (Promega). Different clones were picked for Sanger sequencing. Primers used for 5′ RACE are listed in Table S3.

In Vitro Transcription, Microprocessor, and CPSF3 Cleavage Assays

A T7 primer and gene-specific primers were used to PCR amplify pri-miR-17∼92 sequences from plasmid DNA template. PCR products were gel-purified and used as templates for in vitro transcription using the Riboprobe (Promega) system together with ^{32}P-CTP for radioactive labeling. Microprocessor purified from Flag-DROSHA-293 cells was used for in vitro Microprocessor assays (Gregory et al., 2004). Cold RNA was produced using the same strategy without ^{32}P-CTP addition. For RNA annealing, 10 mM $MgCl_2$ was added to 200 pmol cold RNA and incubated at 95°C for 5 min and then slowly cooled to reverse transcription (RT). Annealed RNA was subjected to 5% native polyacrylamide gel for ethidium bromide staining and used for Microprocessor assay followed by small RNA northern blot analysis. His-CPSF3 complex was purified from *E. coli* as described previously for other proteins (Chang et al., 2013). Assays conditions were as for Microprocessor.

CRISPR/Cas9 Mutagenesis

Oligo DNA (0.5 pmol 200 nt) corresponding to mouse pri-miR-17∼92 sequence containing AG → CC mutation, 12 μg PX330 plasmid containing guide RNA sequence near the cleavage site, and 1 μg plasmid expressing puromycin resistance gene were co-transfected into 3 million V6.5 ESCS by nucleofection using Primary Cell Nucleofector Kits (Lonza). After 1 day, puromycin was added to media. Individual ESC clones were picked and screened by PCR and DNA sequencing.

(E and F) Co-immunoprecipitation (coIP) assays performed by using the indicated Flag-tagged cDNAs, performing Flag-affinity purifications, and analyzing the affinity eluate western blot using indicated antibodies. Where indicated lysates and IPs were treated with RNase A.
(G) CPSF cleavage assays with His-CPSF3 and Flag-ISY1 complex purified from HEK293 cells.
(H) Model for the posttranscriptional control of miR-17∼92 biogenesis.

Synthetic RNA Annealing

Synthetic RNA (from IDT) UUUGGCUUUUUCCUUUUUGUCUA (RD) and UAGAGAAGUAAGGGAAAAUCAAA (RD*) were mixed in buffer (10 mM Tris, pH 8.0, 20 mM NaCl), incubated 95°C 1 min, and cooled slowly to room temperature. Annealed RNA was subjected to 10% native Polyacrylamide Gel for SYBR Gold staining (Invitrogen).

RNase T1 Accessibility Assay

In vitro transcribed RNA was subjected to annealing then incubated with RNase T1 at 37°C for 15 min. Phenol-chloroform was used to isolate the RNA, followed by isopropanol precipitation. Superscript III Reverse Transcriptase (Invitrogen) was used to synthesize cDNA. Pri-miR-17∼92-specific primers were labeled using ^{32}P-ATP T4 and polynucleotide kinase (NEB), followed by Microspin G-50 Columns (GE Healthcare) and products of primer extension subjected to 15% TBE-Urea Polyacrylamide Gel electrophoresis. Primers are listed in Table S3.

Electron Microscopy

RNAs were transcribed using AmpliScribe T7 High Yield Transcription Kit. Transcribed RNAs were gel purified (8% urea polyacrylamide gel). Purified RNA samples were supplemented with 10 mM sodium cacodylate pH 6.8, then heated to 90°C for 30 s and slowly cooled to room temperature. The annealed RNA samples were incubated with 10 mM $MgCl_2$ for 20 min. RNA (2 μl) of 200 ng/μl sample was applied to glow discharged carbon-coated grids. Grids were stained with 2% uranyl acetate. The EM micrographs were collected on a Tecnai G^2 Spirit BioTWIN with Hamamatsu ORCA-HR C4742-95-12HR detector at magnification of 49,000×. Image processing and particle picking was performed using EMAN2 (Tang et al., 2007). Five hundred particles were included for all analysis. Scikit-image was used to measure the diameter and circularity of particles. The results were then plotted using matplotlib.

CoIP and Western Blots

V6.5 ESCs were transfected with pFlag-CMV2 vector expressing AGO2, ISY1, CPSF3, or DGCR8 cDNAs. Cell lysis and coIPs were performed as described before (Mori et al., 2014) and analyzed by western blot using α-Flag (Sigma), α-Drosha (Cell Signaling), α-ISY1 (Abcam), α-CPSF3 (Abcam), and α-CPSF2 (Abcam) antibodies.

Immunoprecipitation and qRT-PCR

HEK293 cells were transfected with pFlag-CMV2 vectors expressing ISY1, CPSF3, or DGCR8. After UV cross-linking, lysates were collected with NETN buffer as described before (Mori et al., 2014). One-tenth of each cell lysate was used for RNA extraction using Trizol reagent (Invitrogen), and the rest was incubated with Anti-Flag M2 Affinity Gel (Sigma-Aldrich) at 4°C overnight. Anti-Flag M2 Affinity Gel was then washed five times using NETN buffer and before RNA extraction with Trizol reagent and analysis by qRT-PCR.

RNA-Affinity Purification and Mass Spectrometry

In vitro-transcribed cold RNA was conjugated to agarose beads and incubated with whole-cell extract from V6.5 ES cells, and the affinity eluate was subjected to SDS-PAGE followed by Coomassie blue staining. Bands were excised and subjected to mass spectrometric sequencing as described before (Chang et al., 2013).

Luciferase Reporter Assays

Dgcr8$^{-/-}$ ESCs were co-transfected with psiCHECK-2 vectors containing mouse pri-miR-17∼92 with the indicated siRNA sequences using Lipofectamine 2000 (Invitrogen). After 2 days of transfection, cells were collected and Passive Lysis Buffer (Promega) added and incubated at RT for 20 min. Dual-Luciferase Reporter Assay System (Promega) was used to measure the Renilla and Firefly activity.

mRNA and miRNA by qRT-PCR

For mRNA analysis, 3 μg total RNA was treated with DNase (Promega) for 2 hr to remove genomic DNA. Superscript III Reverse Transcriptase (Invitrogen) and random primers were used to synthesize cDNA, and IQ SYBR Green Supermix (Bio-Rad) was used to quantify the cDNA. For miRNA analysis, 10 ng total RNA was used. Taqman probes and Universal PCR master mix (Applied Biosystems) were used for cDNA detection. All the primers used for qPCR were listed in Table S4.

ACCESSION NUMBERS

The accession number for the expression profiling of WT, *Dgcr8*$^{-/-}$, and *Dicer*$^{-/-}$ mESCs by high-throughput sequencing reported in this paper is Gene Expression Omnibus: GSE68699.

SUPPLEMENTAL INFORMATION

Supplemental Information includes four figures and four tables and can be found with this article at http://dx.doi.org/10.1016/j.cell.2015.07.008.

AUTHOR CONTRIBUTIONS

P.D. performed all experiments except for the electron microscopy (EM). L.W. and P.S. performed the EM analysis. P.D. and R.I.G. designed all experiments, analyzed data, and wrote the manuscript.

ACKNOWLEDGMENTS

We thank Dr. Andrea Ventura (MSKCC) for providing the *miR-17∼92*$^{-/-}$ ESCs, Dr. Hanno Stein of the Proteomics Center at Boston Children's Hospital for expertise in the microcapillary HPLC and MS, and Dr. Fred Alt's laboratory for advice with CRISPR/Cas9. This work was supported by a grant to R.I.G. from the US National Institute of General Medical Sciences (NIGMS) (R01GM086386) and to P.S. from the National Cancer Institute (R01CA163647).

Received: October 9, 2014
Revised: April 24, 2015
Accepted: June 22, 2015
Published: August 6, 2015

REFERENCES

Bartel, D.P. (2009). MicroRNAs: target recognition and regulatory functions. Cell *136*, 215–233.

Bian, S., Hong, J., Li, Q., Schebelle, L., Pollock, A., Knauss, J.L., Garg, V., and Sun, T. (2013). MicroRNA cluster miR-17-92 regulates neural stem cell expansion and transition to intermediate progenitors in the developing mouse neocortex. Cell Rep. *3*, 1398–1406.

Chakraborty, S., Mehtab, S., Patwardhan, A., and Krishnan, Y. (2012). Pri-miR-17-92a transcript folds into a tertiary structure and autoregulates its processing. RNA *18*, 1014–1028.

Chang, H.M., Triboulet, R., Thornton, J.E., and Gregory, R.I. (2013). A role for the Perlman syndrome exonuclease Dis3l2 in the Lin28-let-7 pathway. Nature *497*, 244–248.

Chaulk, S.G., Thede, G.L., Kent, O.A., Xu, Z., Gesner, E.M., Veldhoen, R.A., Khanna, S.K., Goping, I.S., MacMillan, A.M., Mendell, J.T., et al. (2011). Role of pri-miRNA tertiary structure in miR-17∼92 miRNA biogenesis. RNA Biol. *8*, 1105–1114.

Chaulk, S.G., Xu, Z., Glover, M.J., and Fahlman, R.P. (2014). MicroRNA miR-92a-1 biogenesis and mRNA targeting is modulated by a tertiary contact within the miR-17∼92 microRNA cluster. Nucleic Acids Res. *42*, 5234–5244.

Concepcion, C.P., Bonetti, C., and Ventura, A. (2012). The microRNA-17-92 family of microRNA clusters in development and disease. Cancer J. *18*, 262–267.

Conkrite, K., Sundby, M., Mukai, S., Thomson, J.M., Mu, D., Hammond, S.M., and MacPherson, D. (2011). miR-17∼92 cooperates with RB pathway mutations to promote retinoblastoma. Genes Dev. *25*, 1734–1745.

de Pontual, L., Yao, E., Callier, P., Faivre, L., Drouin, V., Cariou, S., Van Haeringen, A., Geneviève, D., Goldenberg, A., Oufadem, M., et al. (2011). Germline

deletion of the miR-17∼92 cluster causes skeletal and growth defects in humans. Nat. Genet. *43*, 1026–1030.

Di Leva, G., and Croce, C.M. (2010). Roles of small RNAs in tumor formation. Trends Mol. Med. *16*, 257–267.

Dix, I., Russell, C., Yehuda, S.B., Kupiec, M., and Beggs, J.D. (1999). The identification and characterization of a novel splicing protein, Isy1p, of Saccharomyces cerevisiae. RNA *5*, 360–368.

Dominski, Z., Yang, X.C., and Marzluff, W.F. (2005). The polyadenylation factor CPSF-73 is involved in histone-pre-mRNA processing. Cell *123*, 37–48.

Gregory, R.I., Yan, K.P., Amuthan, G., Chendrimada, T., Doratotaj, B., Cooch, N., and Shiekhattar, R. (2004). The Microprocessor complex mediates the genesis of microRNAs. Nature *432*, 235–240.

Guil, S., and Cáceres, J.F. (2007). The multifunctional RNA-binding protein hnRNP A1 is required for processing of miR-18a. Nat. Struct. Mol. Biol. *14*, 591–596.

Ha, M., and Kim, V.N. (2014). Regulation of microRNA biogenesis. Nat. Rev. Mol. Cell Biol. *15*, 509–524.

He, L., Thomson, J.M., Hemann, M.T., Hernando-Monge, E., Mu, D., Goodson, S., Powers, S., Cordon-Cardo, C., Lowe, S.W., Hannon, G.J., and Hammond, S.M. (2005). A microRNA polycistron as a potential human oncogene. Nature *435*, 828–833.

Houbaviy, H.B., Dennis, L., Jaenisch, R., and Sharp, P.A. (2005). Characterization of a highly variable eutherian microRNA gene. RNA *11*, 1245–1257.

Kataoka, N., Fujita, M., and Ohno, M. (2009). Functional association of the Microprocessor complex with the spliceosome. Mol. Cell. Biol. *29*, 3243–3254.

Kim, Y.K., and Kim, V.N. (2007). Processing of intronic microRNAs. EMBO J. *26*, 775–783.

Kyburz, A., Friedlein, A., Langen, H., and Keller, W. (2006). Direct interactions between subunits of CPSF and the U2 snRNP contribute to the coupling of pre-mRNA 3′ end processing and splicing. Mol. Cell *23*, 195–205.

Li, Y., Vecchiarelli-Federico, L.M., Li, Y.J., Egan, S.E., Spaner, D., Hough, M.R., and Ben-David, Y. (2012). The miR-17-92 cluster expands multipotent hematopoietic progenitors whereas imbalanced expression of its individual oncogenic miRNAs promotes leukemia in mice. Blood *119*, 4486–4498.

Lin, S., and Gregory, R.I. (2015). MicroRNA biogenesis pathways in cancer. Nat. Rev. Cancer *15*, 321–333.

Mandel, C.R., Kaneko, S., Zhang, H., Gebauer, D., Vethantham, V., Manley, J.L., and Tong, L. (2006). Polyadenylation factor CPSF-73 is the pre-mRNA 3′-end-processing endonuclease. Nature *444*, 953–956.

Marrone, A.K., Stolz, D.B., Bastacky, S.I., Kostka, D., Bodnar, A.J., and Ho, J. (2014). MicroRNA-17∼92 is required for nephrogenesis and renal function. J. Am. Soc. Nephrol. *25*, 1440–1452.

Mavrakis, K.J., Wolfe, A.L., Oricchio, E., Palomero, T., de Keersmaecker, K., McJunkin, K., Zuber, J., James, T., Khan, A.A., Leslie, C.S., et al. (2010). Genome-wide RNA-mediated interference screen identifies miR-19 targets in Notch-induced T-cell acute lymphoblastic leukaemia. Nat. Cell Biol. *12*, 372–379.

Mendell, J.T. (2008). miRiad roles for the miR-17-92 cluster in development and disease. Cell *133*, 217–222.

Mendell, J.T., and Olson, E.N. (2012). MicroRNAs in stress signaling and human disease. Cell *148*, 1172–1187.

Mori, M., Triboulet, R., Mohseni, M., Schlegelmilch, K., Shrestha, K., Camargo, F.D., and Gregory, R.I. (2014). Hippo signaling regulates microprocessor and links cell-density-dependent miRNA biogenesis to cancer. Cell *156*, 893–906.

Morlando, M., Ballarino, M., Gromak, N., Pagano, F., Bozzoni, I., and Proudfoot, N.J. (2008). Primary microRNA transcripts are processed co-transcriptionally. Nat. Struct. Mol. Biol. *15*, 902–909.

Mu, P., Han, Y.C., Betel, D., Yao, E., Squatrito, M., Ogrodowski, P., de Stanchina, E., D'Andrea, A., Sander, C., and Ventura, A. (2009). Genetic dissection of the miR-17∼92 cluster of microRNAs in Myc-induced B-cell lymphomas. Genes Dev. *23*, 2806–2811.

Nittner, D., Lambertz, I., Clermont, F., Mestdagh, P., Köhler, C., Nielsen, S.J., Jochemsen, A., Speleman, F., Vandesompele, J., Dyer, M.A., et al. (2012). Synthetic lethality between Rb, p53 and Dicer or miR-17-92 in retinal progenitors suppresses retinoblastoma formation. Nat. Cell Biol. *14*, 958–965.

O'Donnell, K.A., Wentzel, E.A., Zeller, K.I., Dang, C.V., and Mendell, J.T. (2005). c-Myc-regulated microRNAs modulate E2F1 expression. Nature *435*, 839–843.

Olive, V., Bennett, M.J., Walker, J.C., Ma, C., Jiang, I., Cordon-Cardo, C., Li, Q.J., Lowe, S.W., Hannon, G.J., and He, L. (2009). miR-19 is a key oncogenic component of mir-17-92. Genes Dev. *23*, 2839–2849.

Olive, V., Sabio, E., Bennett, M.J., De Jong, C.S., Biton, A., McGann, J.C., Greaney, S.K., Sodir, N.M., Zhou, A.Y., Balakrishnan, A., et al. (2013). A component of the mir-17-92 polycistronic oncomir promotes oncogene-dependent apoptosis. eLife *2*, e00822.

Patel, V., Williams, D., Hajarnis, S., Hunter, R., Pontoglio, M., Somlo, S., and Igarashi, P. (2013). miR-17∼92 miRNA cluster promotes kidney cyst growth in polycystic kidney disease. Proc. Natl. Acad. Sci. USA *110*, 10765–10770.

Pawlicki, J.M., and Steitz, J.A. (2010). Nuclear networking fashions pre-messenger RNA and primary microRNA transcripts for function. Trends Cell Biol. *20*, 52–61.

Sandhu, S.K., Fassan, M., Volinia, S., Lovat, F., Balatti, V., Pekarsky, Y., and Croce, C.M. (2013). B-cell malignancies in microRNA Eμ-miR-17∼92 transgenic mice. Proc. Natl. Acad. Sci. USA *110*, 18208–18213.

Siomi, H., and Siomi, M.C. (2010). Posttranscriptional regulation of microRNA biogenesis in animals. Mol. Cell *38*, 323–332.

Tang, G., Peng, L., Baldwin, P.R., Mann, D.S., Jiang, W., Rees, I., and Ludtke, S.J. (2007). EMAN2: an extensible image processing suite for electron microscopy. J. Struct. Biol. *157*, 38–46.

Thornton, J.E., and Gregory, R.I. (2012). How does Lin28 let-7 control development and disease? Trends Cell Biol. *22*, 474–482.

Thornton, J.E., Du, P., Jing, L., Sjekloca, L., Lin, S., Grossi, E., Sliz, P., Zon, L.I., and Gregory, R.I. (2014). Selective microRNA uridylation by Zcchc6 (TUT7) and Zcchc11 (TUT4). Nucleic Acids Res. *42*, 11777–11791.

Ventura, A., Young, A.G., Winslow, M.M., Lintault, L., Meissner, A., Erkeland, S.J., Newman, J., Bronson, R.T., Crowley, D., Stone, J.R., et al. (2008). Targeted deletion reveals essential and overlapping functions of the miR-17 through 92 family of miRNA clusters. Cell *132*, 875–886.

Villa, T., and Guthrie, C. (2005). The Isy1p component of the NineTeen complex interacts with the ATPase Prp16p to regulate the fidelity of pre-mRNA splicing. Genes Dev. *19*, 1894–1904.

Viswanathan, S.R., Daley, G.Q., and Gregory, R.I. (2008). Selective blockade of microRNA processing by Lin28. Science *320*, 97–100.

Wassarman, K.M., and Steitz, J.A. (1993). Association with terminal exons in pre-mRNAs: a new role for the U1 snRNP? Genes Dev. *7*, 647–659.